Supplemental information for Parent material and climate interact to control soil C dynamics through the development of poorly crystalline minerals

Jeffrey Beem-Miller[1], Craig Rasmussen[2], Alison M. Hoyt[1,3], Marion Schrumpf[1], Georg Guggenberger[4], & Susan Trumbore[1]

[1] Department of Biogeochemical Processes, Max Planck Institute for Biogeochemistry, Jena, Germany

[2] Department of Environmental Science, The University of Arizona, Tucson, AZ, USA

[3] Department of Earth System Science Science, Stanford University, Stanford, CA, USA

[4] Institute of Soil Science, Leibniz University Hannover, Hannover, Germany

Supplemental information for Parent material and climate interact to control soil C dynamics through the development of poorly crystalline minerals

Soil carbon

We did not observe clear trends in soil carbon concentration over time for the majority of sites, making us confident that most sites are at steady-state with regards to carbon stock changes (**Fig. 1**). Although we did observe substantial variation in some sites, this is likely due to spatial heterogeneity in soil C concentration that cannot be avoided when destructively resampling the same sites over time (**Fig. 1**). However, we did observe significant trends in soil C concentration with time for a a few of the sites when considered by specific depth increments. However, a caveat is that we did not account for potential differences in the mass of soil sampled over time, as we only considered depth-based increments. We observed significant changes at two sites for the surface layer (0-0.1 m), and at two additional sites in the intermediate depth layer (0.1-0.2 m), but C concentration changes were only significant at a single site showed changes for the deepest depth layer (0.2-0.3 m) (**Table 1**). The soil at the cold climate andesite site was an outlier in that the soil C concentration showed a consistently significant increase in the two deeper depth layers over the study period, while the other soils with significant changes showed decreases in C concentrations (**Table 1**).

Respiration fluxes

SI Figs. 3 and **4**.

Radiocarbon depth profiles: 2001 data

Depth profiles of $\Delta^{14}C_{bulk}$ were similar in 2001 (**SI Fig. 5**) as to what we observed in 2019. We observed the most depleted ^{14}C overall in the cool climate sites, where we also observed the clearest differences among parent materials. Parent material differences were least apparent for the cold climate sites, as we also observed in 2019. Within climate zones

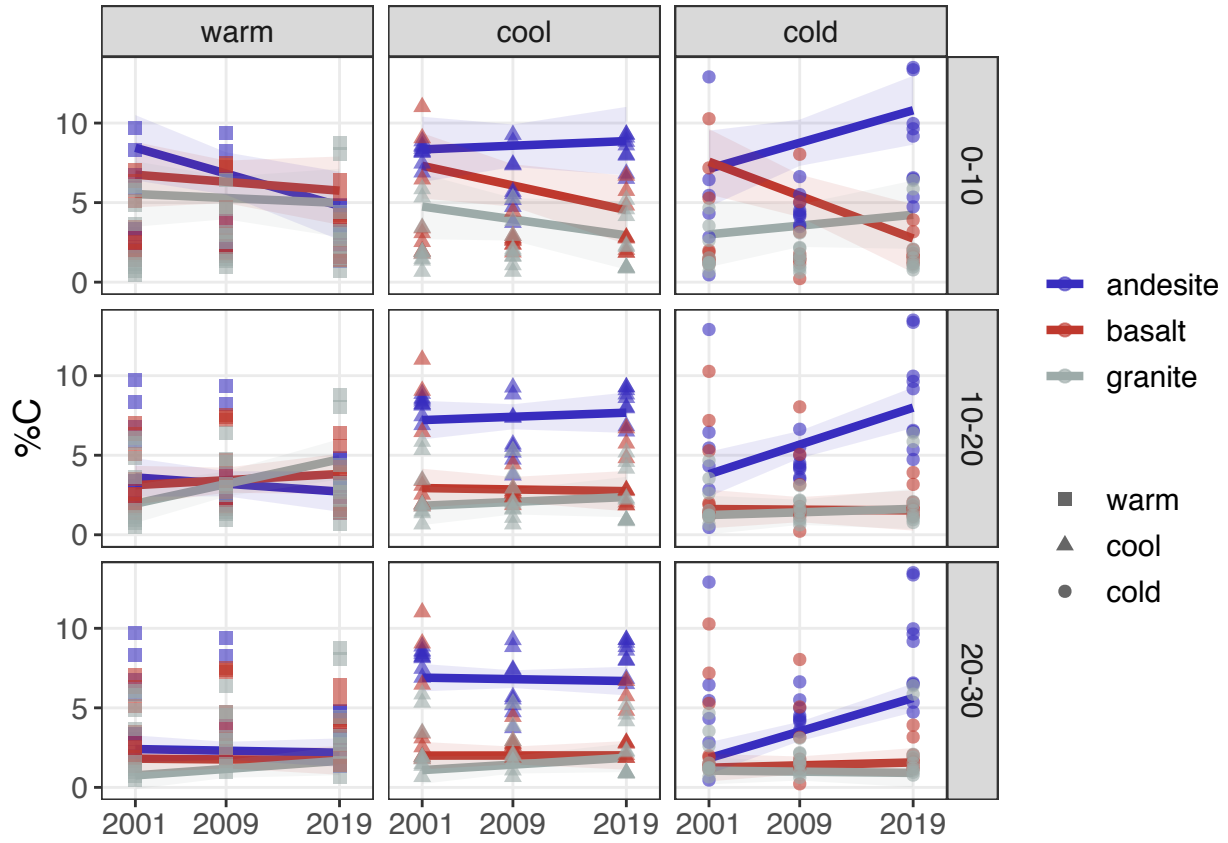

Figure 1. Changes in soil C concentration, 2001-2019. Points show replicate profiles (n = 3); lines show marginal mean estimates of linear trends in soil C concentration with time; ribbons show 95% CIs around trend estimates.

andesitic soils tended be most depleted and the granitic soils most enriched, with the basaltic parent material intermediate between the other two.

Temporal trend analysis

Trends

Please see the main text for discussion of the temporal trends in both $\Delta^{14}C_{bulk}$ and $\Delta^{14}C_{bulk}$. See SI tables **2** and **3** for statistics.

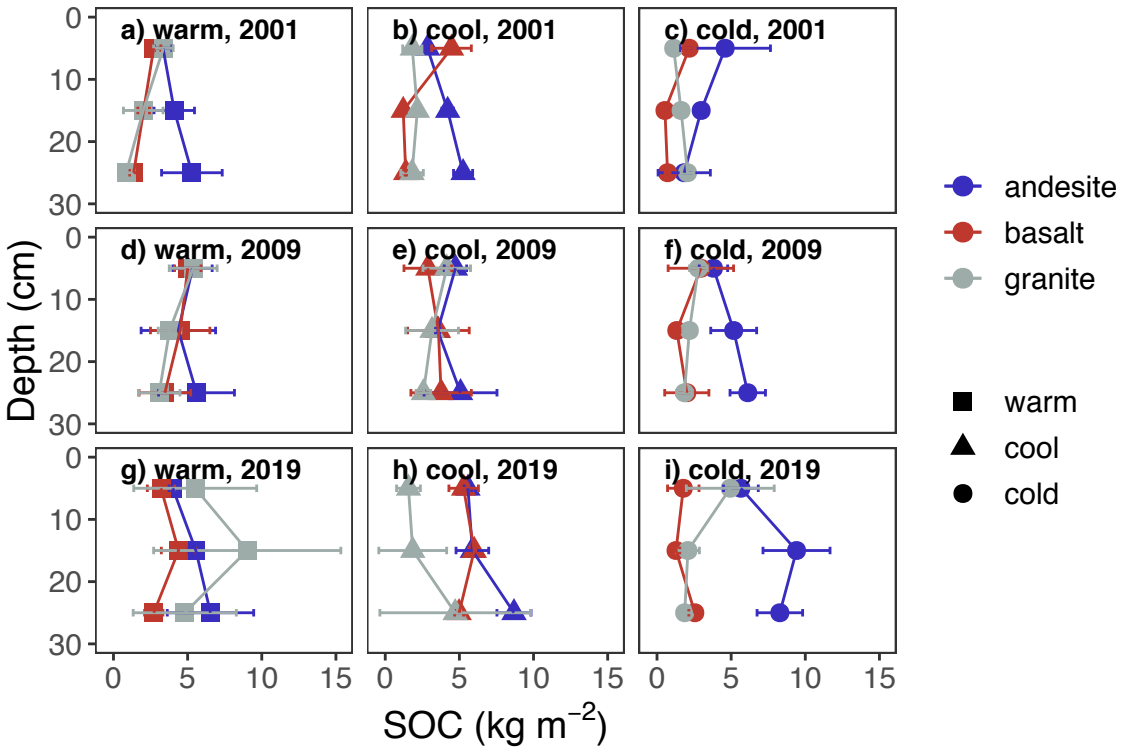

Figure 2. Profiles of soil C stocks by year. Note that bulk density and coarse fragment data were not collected in 2019, so these values were spline-estimated from 2009 data for the 2019 profiles. Points show means; error bars show ±2SE.

Contrasts

We saw more significant contrasts for $\Delta^{14}C_{respired}$ than we did for $\Delta^{14}C_{bulk}$ (**SI Fig. 4**). When considered within climate zones, the basaltic and granitic soils were more similar to one another overall than were either to the andesitic soils. We observed parent material contrasts more commonly in the cool and cold climate sites than in the warm sites; however we only observed significant contrasts for the cold climate sites in the $\Delta^{14}C_{respired}$ data, and not for $\Delta^{14}C_{bulk}$. When considered within parent materials, we saw more siginificant contrasts for the granitic and basaltic soils than for the andesitic soils (**SI Fig. 4**).

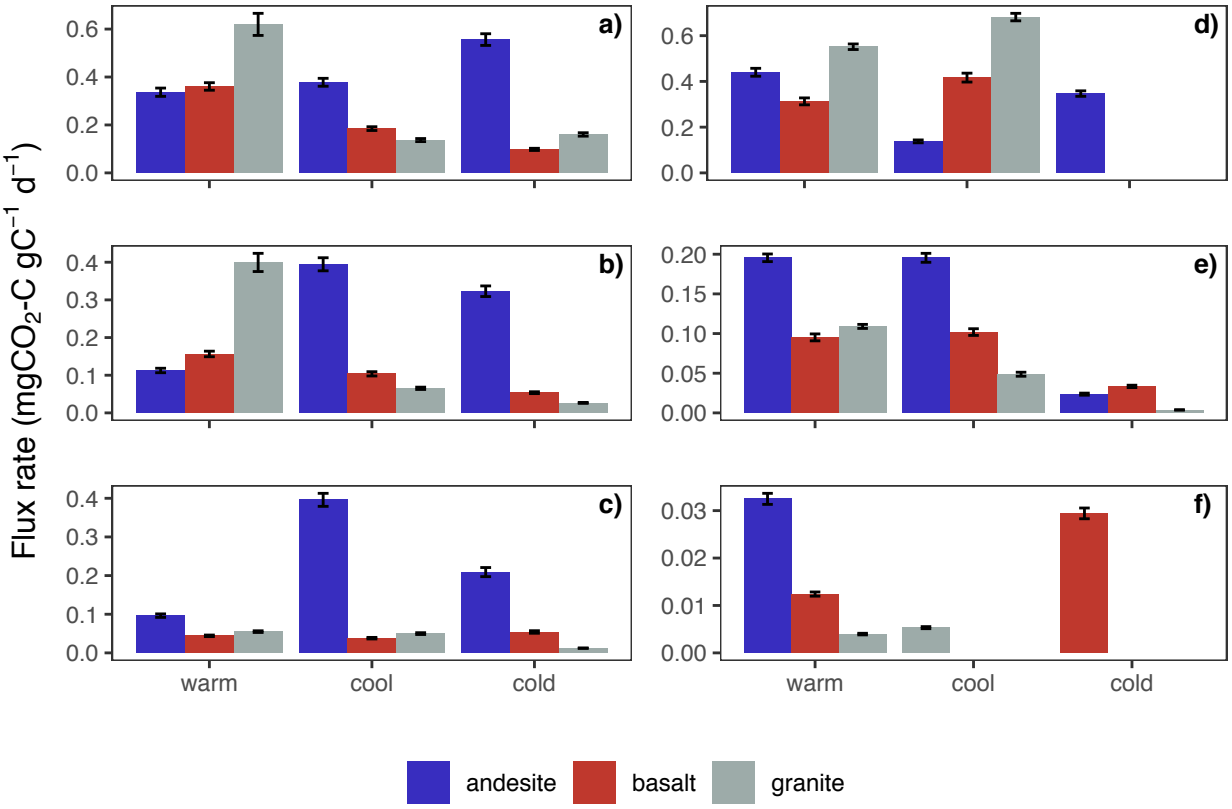

Figure 3. Heterotrophic respiration rates from incubations of 2019 and 2001 samples. Panels a-c show 2019 data, and panels d-f show 2001 data. Panels in the top row (a, d) show the first depth increment for each year, middle row shows the second depth increment (b, e), and the bottom row shows the third depth increment (c, f). Columns show means for laboratory duplicates averaged over the whole incubation period; error bars ± 1 standard error of the mean. NB: Total CO_2 respired was controlled to be within 10,000 ppm (±1,000 ppm) for all samples; incubation duration varied between 4 and 40 days.

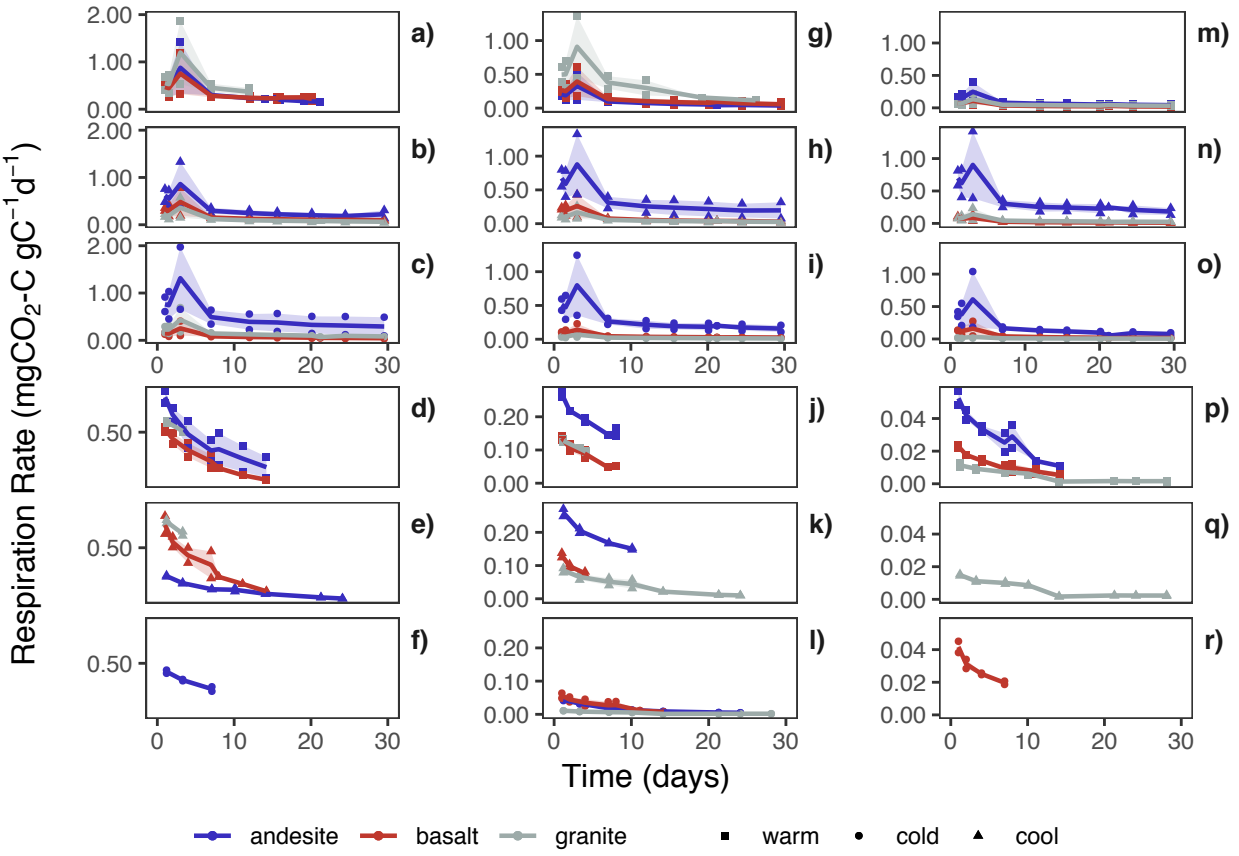

Figure 4. Time series of heterotrophic respiration rates from incubations by depth and year (i.e. samples from the same year and depth interval are plotted on the same scale). Rows correspond to climate zones, columns correspond to depths; leftmost column shows top depth, rightmost column shows deepest depth. Top set of panels (a-c, g-i, and m-o) show 2019 data, bottom set of panels (d-f, j-l, p-r) show 2001 data. Lines show means for laboratory duplicates; ribbon shows minimum and maximum of laboratory duplicates. NB: Total CO_2 respired was controlled to be within 10,000 ppm (±1,000 ppm) for all samples.

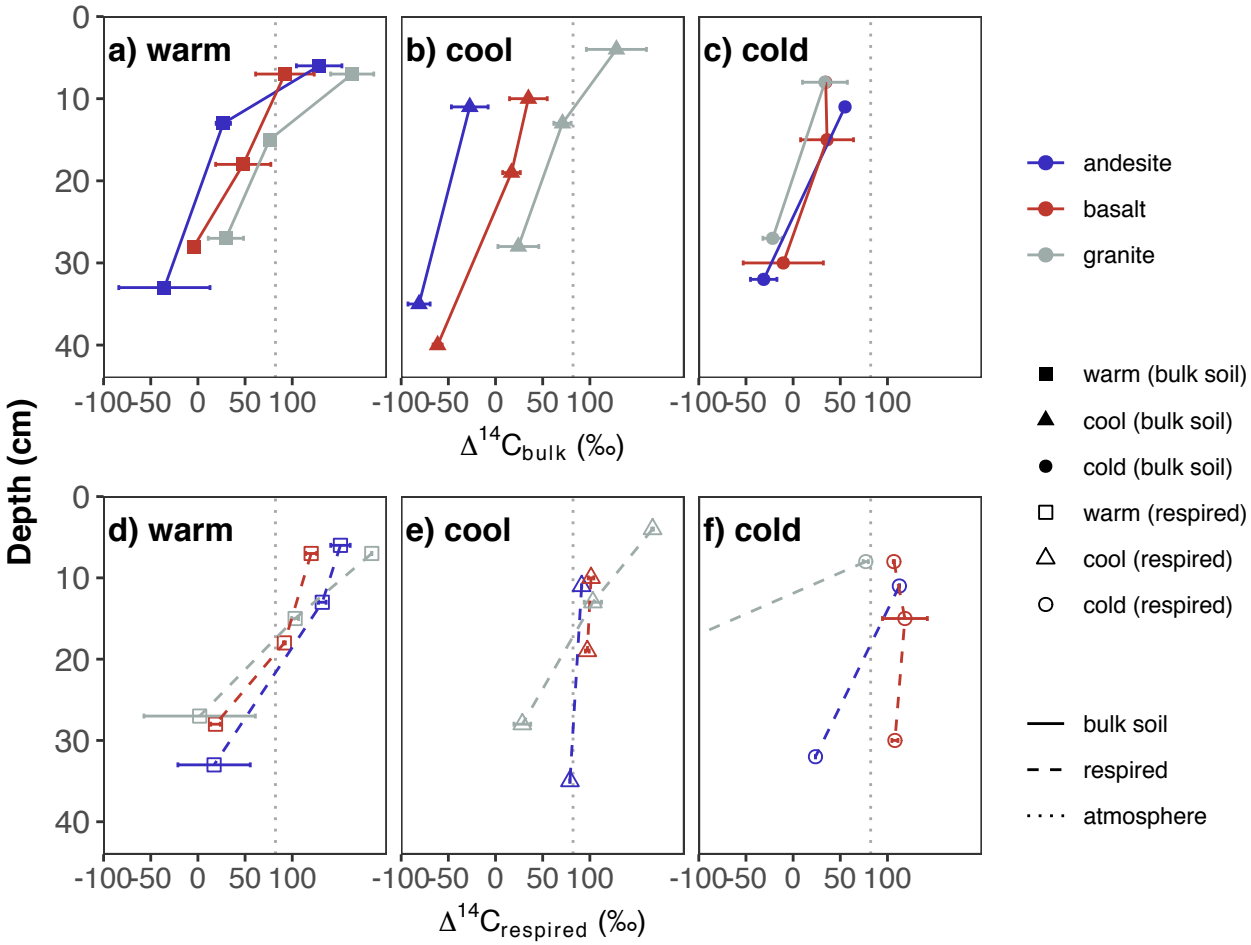

Figure 5. Depth profiles of $\Delta^{14}C_{bulk}$ and $\Delta^{14}C_{respired}$ for 2001 data. Top panels show bulk data, bottom panels respired data. Dotted vertical lines show $\Delta^{14}C$ of the atmosphere in the year of sampling. Points show the mean of three replicate profiles for bulk soil, and the mean of laboratory duplicates for respired CO_2. Error bars show ± 1 SD for bulk soils and the minimum and maximum for respired CO_2. Respired CO_2 from the cold granite site (panel f) was extremely depleted in $\Delta^{14}C$ and thus is excluded for display purposes.

Mineral assemblages

We simplified the data in the main text to consider the relationship between $\Delta^{14}C$ and either poorly crystalline metal oxides or crystalline metal oxides. We present here the individual regression plots for $\Delta^{14}C_{bulk}$ (**SI Fig. 7**) and $\Delta^{14}C_{respired}$ (**SI Fig. 8**).

We also present here the results of the individual regression analyses for $\Delta^{14}C_{respired\text{-}bulk}$ vs. Al selectively dissolved with ammonium oxalate (Al_o) or sodium pyrophosphate (Al_p), and Fe selectively dissolved with ammonium oxalate (Fe_o), or dithionite citrate (Fe_d) **SI Fig. 6**. The relationships for the Al_o, Al_p, and Fe_o models (**Eq. 4**, main text) were all highly significant ($p < 0.001$). Each model explained a similar amount of the variation observed in $\Delta^{14}C_{respired\text{-}bulk}$, with R^2 values of: 0.44, 0.48, 0.55, respectively. The relationship with Fe_d is not significant.

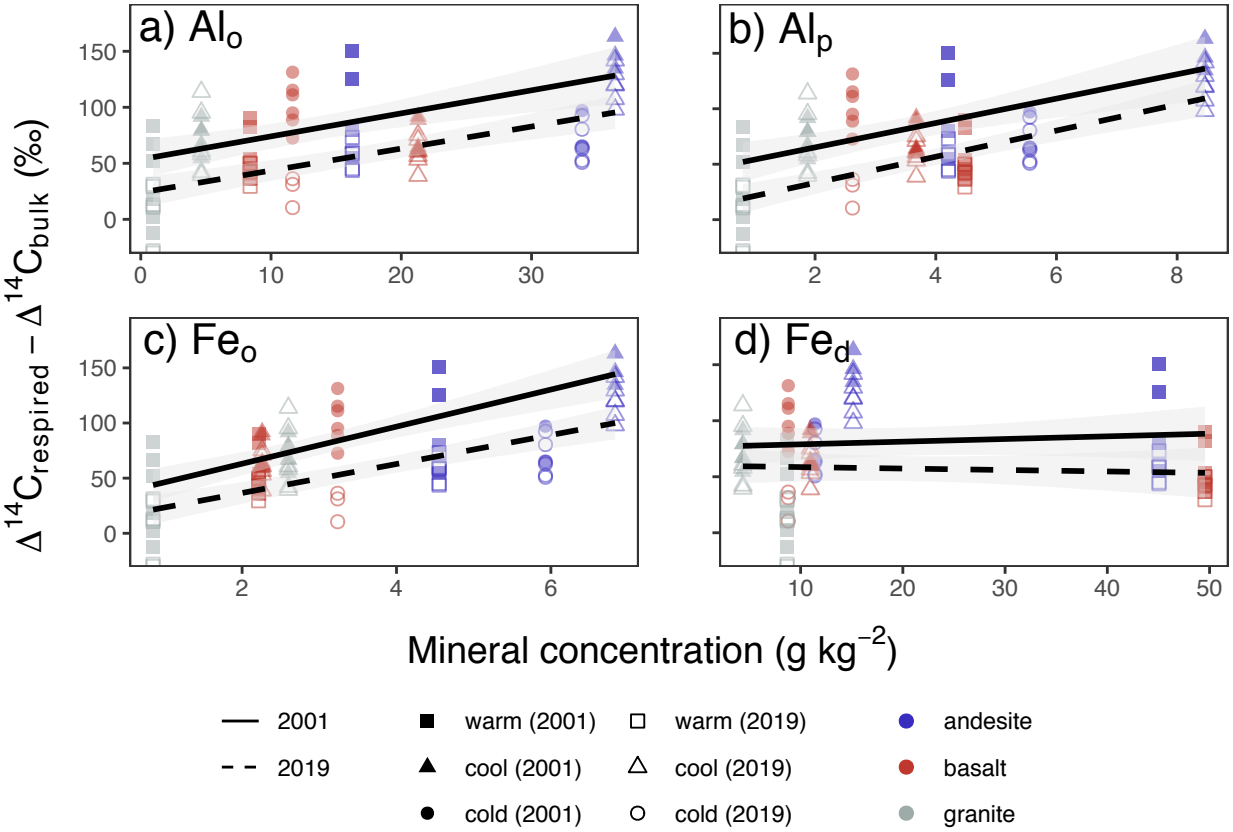

Figure 6. Relationship of selectively dissolved iron and alumnimum to the difference between $\Delta^{14}C_{respired}$ and $\Delta^{14}C_{bulk}$ ($\Delta^{14}C_{respired\text{-}bulk}$). [a)] Oxalate-extractable aluminum (Al_o), [b)] Pyrophosphate-extractable aluminum (Al_p), [c)] Oxalate-extractable iron (Fe_o), [d)] Dithionite extractable iron (Fe_d). Points show mass-weighted mineral concentrations and carbon-weighted values of $\Delta^{14}C_{respired\text{-}bulk}$ for 0-30cm profiles. Lines show linear model fits from **Eq. 5**.

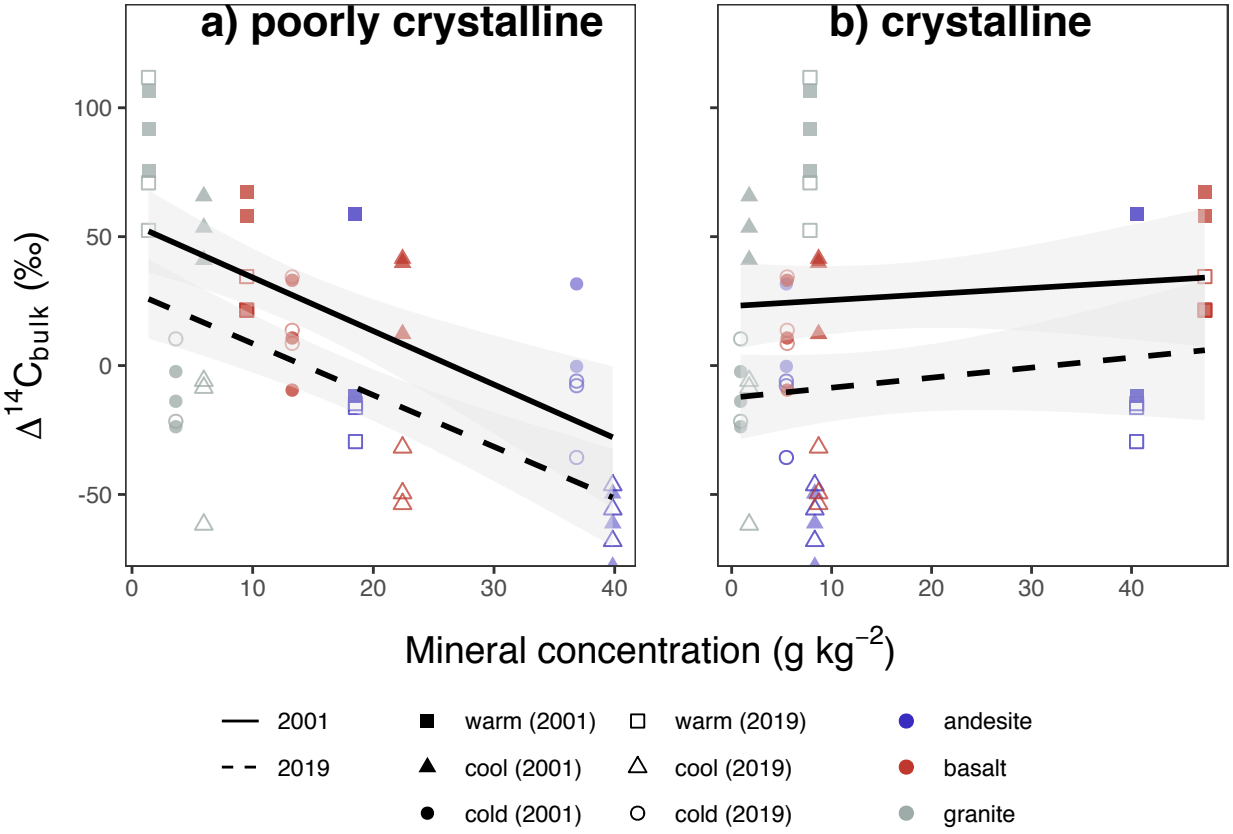

Figure 7. Relationship of poorly crystalline and crystalline minerals to $\Delta^{14}C_{bulk}$. [a)] Poorly crystalline mineral content (oxalate-extractable aluminum + 1/2 oxalate-extractable iron), [b)] Crystalline mineral content (dithionite-extractable iron - oxalate-extractable iron). Points show mass-weighted mineral concentrations and carbon-weighted values of $\Delta^{14}C_{bulk}$ for 0-30cm profiles. Lines show linear model fits from **Eq. 5**.

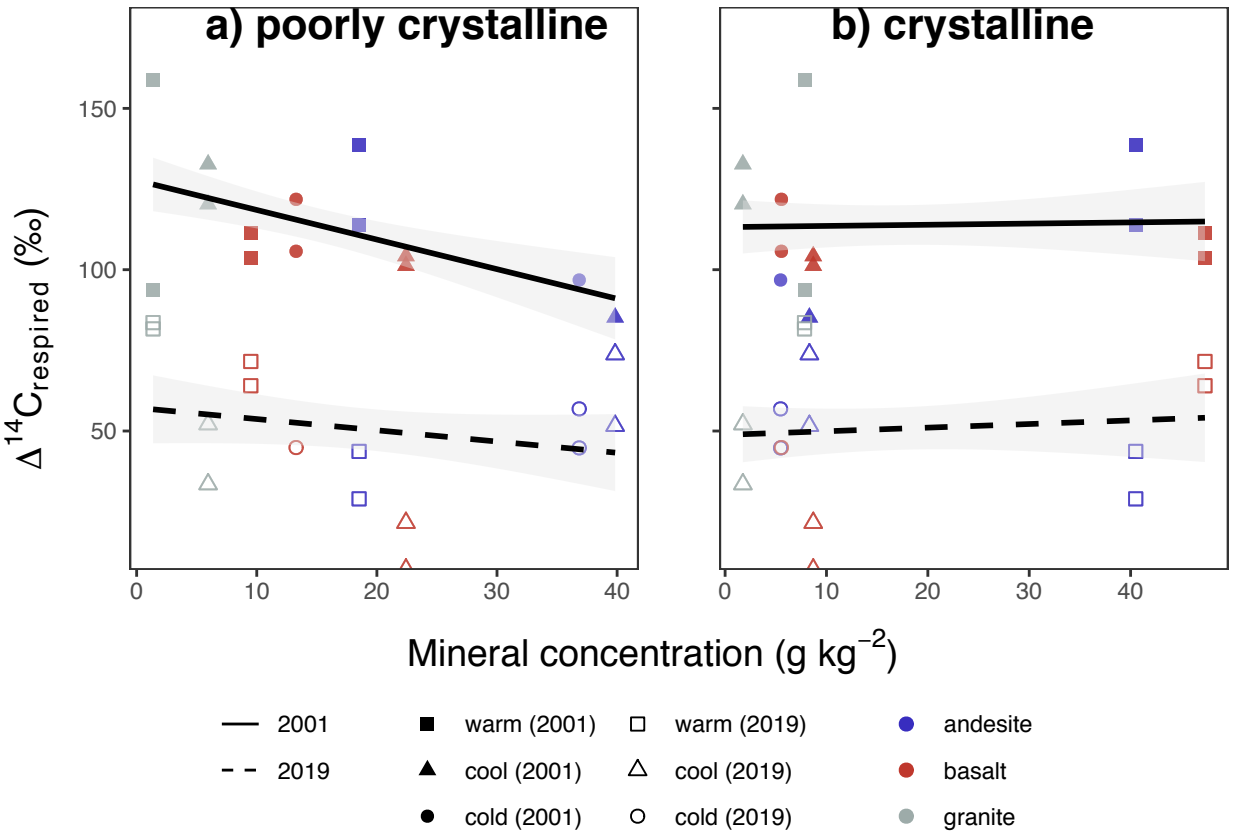

Figure 8. Relationship of poorly crystalline and crystalline minerals to $\Delta^{14}C_{respired}$. [a)] Poorly crystalline mineral content (oxalate-extractable aluminum + 1/2 oxalate-extractable iron), [b)] Crystalline mineral content (dithionite-extractable iron - oxalate-extractable iron). Points show mass-weighted mineral concentrations and carbon-weighted values of $\Delta^{14}C_{respired}$ for 0-30cm profiles. Lines show linear model fits from **Eq. 5** (main text).

Table 1

Changes in soil C concentration (%), 2001-2019. (Only signficant trends shown).

					95% CI	
Depth	Site	Trend	*SE*	df	*lower*	*upper*
0-10cm	andesite (warm)	-0.20	0.09	62	-0.38	-0.02
	andesite (cold)	0.20	0.10	62	0.01	0.40
	basalt (cold)	-0.27	0.09	62	-0.45	-0.09
10-20cm	andesite (cold)	0.23	0.06	62	0.12	0.35
	granite (warm)	0.16	0.05	62	0.05	0.26
20-30cm	andesite (cold)	0.21	0.04	62	0.13	0.29

Table 2

Change in $\Delta^{14}C_{\text{bulk}}$, 2001-2019. Degrees of freedom = 44; confidence level used = 0.95.

		0-10cm		10-20cm		20-30cm	
Climate	Parent material	Trend	*SE*	Trend	*SE*	Trend	*SE*
warm	andesite	**-5.8**	1.0	-1.9	1.3	1.1	1.3
	basalt	-1.8	1.0	-0.1	1.3	-1.1	1.3
	granite	**-2.5**	1.0	2.4	1.3	0.2	1.3
cool	andesite	0.1	1.0	0.4	1.3	0.3	1.3
	basalt	-2.1	1.0	**-3.2**	1.3	**-3.3**	1.3
	granite	**-4.9**	1.0	**-3.5**	1.3	**-3.6**	1.3
cold	andesite	-2.2	1.1	-0.9	1.4	0.4	1.5
	basalt	0.9	1.0	0	1.3	1.4	1.3
	granite	0.1	1.0	0.3	1.3	0.1	1.3

Table 3

Change in $\Delta^{14}C_{\text{respired}}$, 2001-2019. Degrees of freedom = 44; confidence level used = 0.95.

		0-10cm		10-20cm		20-30cm	
Climate	Parent material	Trend	*SE*	Trend	*SE*	Trend	*SE*
warm	andesite	**-6.2**	1.0	-2.1	1.0	1.4	2.0
	basalt	**-2.3**	1.0	-0.9	1.0	0.4	2.0
	granite	**-3.7**	1.0	2	1.0	3.2	2.0
cool	andesite	-1.4	1.2	-1	1.2	-1.5	2.5
	basalt	**-3.7**	1.0	**-5.9**	1.0	NA	NA
	granite	**-3**	1.0	**-4.1**	1.0	0	2.0
cold	andesite	**-2.9**	1.2	-0.8	1.2	1.4	2.5
	basalt	**-3.9**	1.0	**-3.9**	1.0	-3.5	2.5
	granite	0.1	1.0	**4.8**	1.4	NA	NA

Table 4

Contrasts for bulk and respired $\Delta^{14}C$ temporal trends. P value adjustment: Tukey method for comparing a family of 3 estimates.

			Bulk			Respired		
Depth	Group	Contrast	Est.	*SE*	*p*	Est.	*SE*	*p*
0-10cm	warm	andesite - basalt	-4.0	1.4	**0.021**	-3.9	1.4	**0.036**
	warm	andesite - granite	-3.3	1.4	0.068			
	cool	andesite - granite	5.0	1.4	**0.004**			
	cold	basalt - granite				-4.0	1.4	**0.031**
	andesite	warm - cool	-5.9	1.4	**< .001**	-4.8	1.6	**0.021**
	andesite	warm - cold	-3.6	1.5	0.06			
	granite	warm - cold				-3.7	1.4	**0.045**
	granite	cool - cold	-5.0	1.4	**0.004**			
10-20cm	warm	andesite - granite	-4.3	1.8	0.051	-4.1	1.4	**0.03**
	cool	andesite - basalt				4.9	1.6	**0.019**
	cool	andesite - granite	4.0	1.8	0.08			
	cold	andesite - granite				-5.6	1.9	**0.024**
	cold	basalt - granite				-8.7	1.7	**< .001**
	basalt	warm - cool				5.0	1.4	**0.008**
	granite	warm - cool	5.9	1.8	**0.005**	6.1	1.4	**0.002**
	granite	cool - cold	-3.8	1.8	0.094	-8.9	1.7	**< .001**
20-30cm	basalt	cool - cold	-4.7	1.9	**0.04**			